Macromolecules

pubs.acs.org/Macromolecules Article

Thermodynamic Interactions in Polydiene/Polyolefin Blends Containing Diverse Polydiene and Polyolefin Units

Jialin Qiu, Xuejian Chen, Amy N. Le, Carlos R. López-Barrón, Brian J. Rohde, Ronald P. White, Jane E. G. Lipson, Ramanan Krishnamoorti, and Megan L. Robertson

Cite This: *Macromolecules* 2023, 56, 2286−2297

ABSTRACT: Thermodynamic interactions were investigated in blends of melts containing 1,4-polyisoprene (1,4-PI) and copolymers of 1,2-polybutadiene (1,2-PBD), poly(ethyl ethylene) (PEE), and/or polyethylene (PE) units. Specifically, two classes of blends were examined: one contained the polydiene 1,4-PI and a diene-olefin copolymer of 1,2-PBD and PEE units (1,2-PBD-*co*-PEE, with the PEE volume fraction varying from 0 to 1), and the other contained 1,4-PI and a fully olefinic copolymer of PE and PEE units (PE-*co*-PEE, with the PEE volume fraction varying from 0.05 to 1). The Flory−Huggins interaction parameter, χ, was measured using small-angle neutron scattering (SANS) for homogeneous blends at or close to their critical compositions. SANS data were analyzed through the Zimm method and fitting of the random phase approximation model to extract $\chi(T)$. Random copolymer theory (RCT) was applied to understand the resulting $\chi(T)$ behavior. In 1,2-PBD-*co*-PEE/1,4-PI blends, predictions using the RCT model showed excellent agreement with the measured $\chi(T)$, indicating the presence of random mixing and dominance of dispersive forces in these blends. By contrast, RCT failed to describe the $\chi(T)$ behavior in PE-*co*-PEE/1,4-PI blends. The PE-*co*-PEE/1,4-PI blends were further examined using lattice cluster theory and solubility parameter formalism, yet neither approach could explain the $\chi(T)$ behavior. The locally correlated lattice model, which correlates the equation of state properties with the polymer blend miscibility, was found to reasonably describe the phase behavior of PE-*co*-PEE/1,4-PI blends.

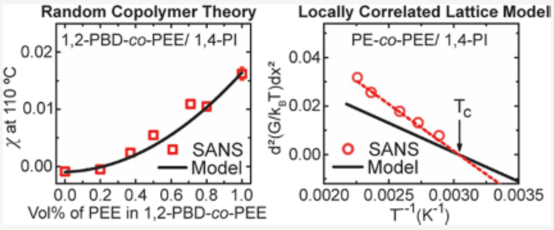

1. INTRODUCTION

The Flory−Huggins interaction parameter, χ, is the characteristic parameter describing thermodynamic interactions in multicomponent polymer systems such as polymer blends (in their melt state) and governs important blend properties such as miscibility, interfacial width, and mechanical properties.[1−4] We previously demonstrated that mixtures of polydienes and polyolefins, with commercial applicability in products such as elastomers and sealants, exhibited unusually large and strongly temperature-dependent χ parameters.[5] These strong interactions could be modulated when olefinic repeat units were introduced into the polydiene (through partial saturation of the polymer, forming a polydiene-polyolefin random copolymer). In those cases, χ of the polyolefin-polydiene copolymer/polyolefin blends decreased with increasing olefin content in the copolymer.[6]

Random copolymer theory (RCT) is traditionally applied to understand χ in blends containing random copolymers, in which χ depends on the copolymer composition. In a blend of copolymers A_xB_{1-x} and C_yD_{1-y}, χ is described as:

$$\chi = \ y\chi_{AC} \quad 1 - \ \ )\ 1 - y)\chi_{BD} \quad 1 - y)\chi_{AD}$$
$$1 - \ \ )y\chi_{BC} - \quad 1 - \ \ )\chi_{AB} - y\ 1 - y)\chi_{CD} \qquad (1)$$

where x and y are the volume fractions of A and C in the random copolymers A_xB_{1-x} and C_yD_{1-y}, respectively, and χ_{ij} are the segment−segment interaction parameters among copolymer components A, B, C, and D.[7−10] This theory assumes that contacts between molecules are random and only proportional to their volume fractions in the copolymers, as well as the presence of dispersive forces only, and therefore lack of specific interactions. Simple blends with weak interactions and/or nonspecific interactions are well described by the RCT;[11−14] in other blends, with strong and/or specific interactions such as hydrogen bonding, there are significant departures.[15,16] Typically, these departures are observed in conjunction with nonrandom mixing, copolymer sequence distribution effects, and/or non-mean-field behavior.

Previously, we explored χ in polydiene-polyolefin copolymer/polyolefin blends composed of one polydiene component and one polyolefin component: 1,2-polybutadiene-*co*-poly(ethyl ethylene) (1,2-PBD-*co*-PEE) blended with PEE and

Received: September 7, 2022
Revised: December 15, 2022
Published: March 7, 2023

https://doi.org/10.1021/acs.macromol.2c01866
Macromolecules 2023, 56, 2286−2297

1,4-polyisoprene-*co*-poly(ethylene-*alt*-propylene) (1,4-PI-*co*-PEP) blended with PEP.[6] Even though the polydiene/polyolefin interactions in these blends were strong (i.e., $\chi_{1,2\text{-PBD/PEE}}$ and $\chi_{1,4\text{-PI/PEP}}$ were large as compared to that in systems of only polyolefins or only polydienes), the RCT could capture the copolymer composition dependence of $\chi(T)$ in these blends, implying random mixing. However, thermodynamic interactions in copolymer/homopolymer blends containing diverse polydiene and polyolefin units are still underexplored.

Previous studies demonstrated that $\chi(T)$ of polydiene copolymer blends containing more than one type of diene (e.g., copolymers of PBD with differing microstructures) has generally been well described by RCT.[12,17−19] Similarly, blends of copolymers containing more than one type of polyolefin (e.g., saturated polybutadienes of differing microstructures) have also behaved consistently with the expectations of RCT.[14] One notable example of a polyolefin copolymer blend that was not described adequately by RCT is a polyethylene (PE)/PEE system in which copolymer thermodynamic interactions (and the measured PVT properties) varied nonlinearly with the PE-*co*-PEE copolymer microstructure.[16] An open question remains as to whether RCT can generally be applied to describe the thermodynamic interactions in random copolymer blends containing multiple polydiene and polyolefin components.

Here, we examine thermodynamic interactions in two copolymer/homopolymer systems containing diverse polydiene and polyolefin components. We identified the components of these blends based on literature studies showing cases where RCT succeeded and failed in polydiene or polyolefin systems. In the first system, we built upon the prior knowledge that RCT successfully described the thermodynamic interactions in 1,2-PBD-*co*-1,4-PBD/1,4-PI blends,[18] and we therefore incorporated 1,2-PBD in a polydiene-polyolefin copolymer (1,2-PBD-*co*-PEE) and blended this copolymer with the polydiene 1,4-PI. In the second system, we chose a polyolefin copolymer system where the RCT failed in PE-*co*-PEE copolymer blends[16] and blended PE-*co*-PEE with the polydiene 1,4-PI. For both systems, small-angle neutron scattering (SANS) data were analyzed through Zimm and random phase approximation (RPA) analyses to quantify $\chi(T)$ for each system at various copolymer compositions. The dependence of χ on copolymer composition and temperature and resulting phase behavior were examined with various theories, including RCT, lattice cluster theory (LCT), solubility parameter formalism, and the locally correlated lattice (LCL) model.

2. EXPERIMENTAL DETAILS

2.1. Polymer Synthesis. *2.1.1. Anionic Polymerization of 1,3-Butadiene and Isoprene.* Our protocols for the synthesis of 1,4-PI and 1,2-PBD have been previously published.[5,6] Briefly, 1,4-PI and 1,2-PBD were synthesized through anionic polymerization with *sec*-butyllithium as the initiator. 1,3-Butadiene (≥99%, Sigma-Aldrich) and isoprene (≥99%, Sigma-Aldrich) were purified over calcium hydride (CaH_2, ≥95%, Sigma-Aldrich) followed by *sec*-butyllithium (1.4 M in cyclohexane, Sigma-Aldrich) for 1,3-butadiene and *n*-butyllithium (2.0 M in cyclohexane, Sigma-Aldrich) for isoprene. For the synthesis of 1,2-PBD, 1,2-diperidioethane (DIPIP, synthesized according to ref 20) was added with 10:1 DIPIP:*sec*-butyllithium molar ratio. The polymerization reactions were conducted at 0 °C for 1,2-PBD and 20 °C for 1,4-PI under 5 psi argon pressure in cyclohexane.

For the synthesis of 1,4-PBD-*co*-1,2-PBD copolymers, the 1,3-butadiene monomer was purified over calcium hydride and *sec*-butyllithium following ref 5. THF (≥99.8%, J.T. Baker) was used as an additive to adjust the %1,2-content of the 1,4-PBD-*co*-1,2-PBD copolymers. THF was distilled from CaH_2 before adding to the reaction mixture. The percent of 1,2-addition was not only dependent on the ratio of THF to *sec*-butyllithium but also the *sec*-butyllithium concentration. A calibration curve of %1,2-content as a function of mol THF:mol *sec*-butyllithium at different *sec*-butyllithium concentrations is shown in Figure S1. The desired volume of THF was measured and transferred into a flame-dried ampule inside the glovebox. The ampule containing THF was then attached to a multineck reactor containing a pressure gauge and pressure relief valve. Preparation of the initiator and cyclohexane solvent was detailed in our earlier publication.[5] Flasks containing monomer, initiator, and cyclohexane were connected to the reactor. The reactor was purged with argon gas and degassed following procedures in ref 5. The polymerization reactions were conducted at 0 °C under 5 psi argon pressure in cyclohexane. The reaction time varied from 3 to 48 h depending on the desired molecular weight. The reaction was terminated using dried isopropanol (≥99.5%, Sigma-Aldrich), and the polymer was precipitated in a 50/50 mixture of methanol (≥99.8%, VWR Chemicals BDH)/acetone (≥99.5%, VWR Chemicals BDH). After most of the solvent was evaporated in a fume hood, the polymers were dried at 40 °C in a vacuum oven for 2 weeks until they reached a constant weight. Deuterated 1,4-PI (d1,4-PI) was purchased from Polymer Source.

2.1.2. Preparation of 1,2-PBD-co-PEE and PE-co-PEE through Saturation of 1,2-PBD and 1,4-PBD-co-1,2-PBD. Procedures for the saturation of 1,2-PBD were previously published in refs 5 and 6. For the partial saturation of 1,2-PBD (forming 1,2-PBD-*co*-PEE copolymers), the catalyst was composed of chlorotris-(triphenylphosphine)rhodium(I) (commonly known as Wilkinson's catalyst, 99%, Strem Chemical) and triphenylphosphine (PPh_3, 99%, Sigma-Aldrich), with an adjustable catalyst-to-polymer ratio depending on the targeted saturation level. For saturation levels lower than 25%, the molar ratio of 1,2-PBD:Wilkinson's catalyst:PPh_3 was 450:1:19. For saturation levels higher than 25%, the molar ratio of 1,2-PBD:Wilkinson's catalyst:PPh_3 was 450:19:1. The reactor was purged with argon followed by charging with 500 psi H_2 or D_2 pressure and heating at 90 °C. The reaction time varied from 2 to 24 h. The reaction kinetics were monitored and published in our earlier paper.[6]

For full saturation of 1,2-PBD (forming PEE), a Pd catalyst (5% on $BaSO_4$, unreduced, Strem Chemical) with a ratio of 1 g catalyst per 1 g polymer was employed. The reactor was purged with argon followed by charging with 500 psi H_2 or D_2 pressure and heating at 90 °C. The reaction was conducted for 48 h, followed by removal of the catalyst and addition of fresh catalyst. The reaction was then conducted for an additional 48 h until a saturation level higher than 99% was attained.

PE-*co*-PEE copolymers were synthesized through the saturation of 1,4-PBD-*co*-1,2-PBD copolymers. The Pd catalyst was used to achieve full saturation of 1,4-PBD-*co*-1,2-PBD with a ratio of 1 g catalyst per 1 g polymer. The saturation reaction proceeded in a Parr high-pressure reactor using the protocol of full saturation of 1,2-PBD described above and in our earlier publications.[5,6] Briefly, the reactor was purged with argon followed by charging with 500 psi H_2 or D_2 pressure and heating at 90 °C. The catalyst was removed after an initial reaction of 48 h. Fresh catalyst was added, followed by another 48 h reaction until a saturation level higher than 99% was attained.

For saturation procedures employing Wilkinson's catalyst, the catalyst was removed through column chromatography using silica gel and cyclohexane, with details described in our earlier paper.[6] Multiple column purifications were required until clear and colorless polymers were attained. For saturation procedures employing the Pd catalyst, the catalyst was removed by filtration using a stack of four paper filters (in the order of 11, 8, 11, and 8 μm). The final solution was filtered using a 0.2 μm filter. For all polymers, after most of the solvent was evaporated in a fume hood, the polymers were dried at 40 °C in a vacuum oven for 2 weeks until the sample reached a constant weight.

2.2. Polymer Characterization. *2.2.1. Nuclear Magnetic Resonance (NMR).* ^{1}H NMR was used to characterize the microstructure of the unsaturated polymers (Figures S2−S6) using a JEOL ECA-500 instrument, employing a solution with a concentration of 29 mg/mL in deuterated chloroform (99.8% D, Cambridge Isotope Laboratories, Inc.). Carbon NMR (^{13}C NMR) experiments to probe monomer sequence distribution in copolymers (Figure S7) were performed on a JEOL ECA-600 instrument with a solution polymer concentration of 214 mg/mL in deuterated chloroform and 15 mg/mL chromium acetyl acetonate as the relaxation agent. The relaxation delay time was set at 3.6 s for ^{13}C NMR experiments to ensure that the molecules were fully relaxed for quantitative results. For ^{13}C NMR, the nuclear Overhauser effect (NOE) was turned off and data were collected overnight to ensure a signal-to-noise ratio greater than 250:1. Chemical shifts were referenced to the proton and carbon resonances of chloroform at 7.26 and 77.36 ppm, respectively.

2.2.2. Gel Permeation Chromatography (GPC). GPC was used to characterize the weight average molecular weight (M_w) and dispersity ($Đ$, defined as M_w/M_n, where M_n is the number average molecular weight) (Figures S8−S14). THF was used as the mobile phase with the flow rate maintained at 1 mL/min at 30 °C. The sample concentration was 1−5 mg/mL and injected to the column at 100 μL injection volume. The eluted samples were analyzed using three detectors: differential refractometer, viscometer, and light scattering. Light scattering was performed with a laser of wavelength of 670 nm. The change in refractive index with concentration (dn/dc) was measured using the refractometer. The dn/dc values measured in THF at 30 °C for 1,2-PBD and 1,4-PI were 0.1050 ± 0.0002 and 0.1381 ± 0.0007, respectively. For 1,4-PBD-*co*-1,2-PBD with %1,2 ranging from 5 to 79%, dn/dc was measured in the range of 0.1357 ± 0.0009 to 0.1133 ± 0.0007 (in THF at 30 °C).

2.2.3. Density Measurement. A density gradient column was used to characterize the density of polymers at 23 °C as described in our earlier paper.[5] The number of deuterium atoms per repeat unit, n_D, was calculated as follows,

$$n_D = \frac{M_{0,H} \ \frac{\rho_D}{\rho_H} - 1)}{m_D - m_H) \quad M_{0,H} \ \frac{\rho_D}{\rho_H}) \ \frac{\beta}{2})} \qquad (2)$$

where $M_{0,\,H}$ is the molecular weight of the hydrogenated species, ρ_D and ρ_H are the densities of the deuterated and hydrogenated polymers, respectively, m_D and m_H are the atomic weights of deuterium and hydrogen, β is the fractional reduction in molar volume for full replacement of hydrogen with deuterium, taken as an average value of 0.002 for saturated hydrocarbon materials,[14,21−23] and $2H$ is the number of hydrogen atoms in a repeat unit of the hydrogenated polymers (where the repeat unit is defined such that $2H$ = 8 in our study).

2.2.4. Polymer Characteristics. The microstructure and molecular weight characteristics of polymers used in this study are provided in Tables 1 and 2.

2.2.5. Blend Preparation. The polymer components of the blends were codissolved in cyclohexane at room temperature at the critical composition (calculated using Flory−Huggins theory). The blend solution was solvent-cast onto a quartz window mounted in a 1 mm spacer titanium cell designed by the National Institute of Standards and Technology (NIST). The majority of the solvent was evaporated in a fume hood followed by drying at 40 °C in a vacuum oven for 1 week until fully dry. The samples were capped with a second quartz window. Table 3 shows the blend characteristics.

Table 1. Polymer Characteristics of 1,4-PI, 1,2-PBD, and PEE

polymer[a]	M_w (kg/mol)[b]	$Đ$[b]	%1,4 in PI or 1,2 in PBD[c]	ρ (g/mL) at 23 °C[e]	N_{rpt} at 23 °C[f]	n_D[g]
1,4-PI-2k	1.9	1.04	94.1	0.8957	37	
1,4-PI-3k	3.4	1.10	94.0	0.9016	63	
1,4-PI-4k	3.8	1.17	94.0	0.9190	73	
1,4-PI-11k	11	1.04	94.1	0.9016	211	
d1,4-PI-3k	3.2	1.14	94.1	0.9747	55	6.15
d1,4-PI-23k	23	1.16	94.0[d]	0.9857	384	6.25
1,2-PBD-47k	47	1.04	99.2	0.8868	871	
dPEE-3k	3.4	1.01	98.6	0.9143	68	3.10
hPEE-5k	5.1	1.01	98.6	0.8657	98	

[a] 1,4-PI-*X*k refers to 1,4-PI with M_w of *X* kg/mol, and the prefix d indicates that the polymer was deuterated. 1,2-PBD-*X*k refers to 1,2-PBD with M_w of *X* kg/mol. (h/d)PEE-*X*k refers to PEE (obtained by saturation of 1,2-PBD with H_2 or D_2) with M_w of *X* kg/mol, which is either hydrogenous (h) or deuterated (d). [b] Measured using GPC with triple detection (polyolefins: measured for the polydiene precursor). [c] %1,2-addition of PBD or 1,4-additon of 1,4-PI (polyolefins: measured for the polydiene precursor). Measured through ^{1}H NMR; error estimated at ±0.4−0.9%. [d] Deuterated 1,4-PI was purchased from Polymer Source with %1,4 content provided by the supplier. [e] Measured using a density gradient column. The error was quantified to be less than ±0.0003 mL through measurements on multiple samples, employing multiple density gradient columns. [f] Number of repeat units per chain at 23 °C based on the reference volume of 100 Å^3. An average thermal expansion coefficient of 0.00068 K^{-1} was used for the polymers to account for the temperature dependence of the molar volume.[24,25] [g] The number of deuterium atoms per repeat unit was calculated using eq 2.

2.2.6. Small-Angle Neutron Scattering (SANS). SANS contrast was induced through saturation of 1,2-PBD with D_2, saturation of 1,4-PBD-*co*-1,2-PBD copolymers with D_2, or use of deuterated 1,4-PI (d1,4-PI) purchased from Polymer Source. SANS experiments were carried out on the NG-7 30m SANS, NGB 30m SANS, and NG-3 VSANS beamlines at the NIST Center for Neutron Research. On the NG-7 and NGB 30m beamlines, the neutron wavelength (λ) was 6 Å and resolution $\Delta\lambda/\lambda$ values were 0.11−0.22 (NG-7) and 0.1−0.3 (NGB). The sample-to-detector distances were 13, 4, and 1 m for experiments on these two beamlines, resulting in a wavevector magnitude (q), $q = (4\pi/\lambda)\sin(\theta/2)$ (where θ is the scattering angle), ranging from 0.003 to 0.5 Å^{-1}. On the NG-3 VSANS beamline, two configurations were used. In one configuration, λ = 6 Å and $\Delta\lambda/\lambda$ = 0.11 − 0.22, with sample-to-detector distances of 9.1 and 2.1 m; a second configuration with λ = 6.7 Å and $\Delta\lambda/\lambda$ = 0.12 was employed with sample-to-detector distances of 21.1 and 4.1 m. These two configurations on NG-3 allowed for accessing a q range of 0.003 to 0.5 Å^{-1}. A 7-position heating block with cartridge heaters was used. The SANS intensity was corrected for detector sensitivity, background, empty cell, sample transmission, and sample thickness.[26] The incoherent background (I_{inc}) was quantified as the plateau value of I_{total} at high q, determined as the slope of $I_{total}q^4$ vs q^4, over a q range of 0.25−0.35 Å^{-1}, as previously reported.[5] The blends that were cloudy at room temperature were heated to the homogeneous state and equilibrated for 1 h before collecting data. The uncertainty in $I_{coh}(q)$ was provided by the beamline for each measurement of I_{coh}.

2.3. SANS Data Analysis. *2.3.1. Zimm Method.* SANS data were analyzed using the Zimm method to extract χ following our previously published protocols.[5,6] A linear dependence of $1/I_{coh}(q)$ vs q^2 is anticipated when $qR_g < 0.7$, and χ was quantified from the value of $1/I_{coh}(q \rightarrow 0)$ obtained from this plot, as described previously.[5,6]

2.3.2. Random Phase Approximation (RPA) Model. SANS data, $I(q)$ vs q, were analyzed through fitting with the RPA model to extract χ(T) and chain dimensions of the blend components following refs 5 and 6. A chain expansion factor, , was applied to allow for variation of the radius of gyration, R_g, in the presence of the other blend components:

Table 2. Polymer Characteristics of 1,2-PBD-*co*-PEE and PE-*co*-PEE

polymer[a]	vol % PEE[b]	M_w (kg/mol)[c]	$Đ$[c]	% 1,2 in PBD[d]	ρ (g/mL) at 23 °C[e]	N_{rpt} at 23 °C[f]	n_D[g]
1,2-$PBD_{0.2}$-*co*-$dPEE_{0.8}$-47k	80	47	1.04	99.2	0.9008	909	1.60
1,2-$PBD_{0.29}$-*co*-$dPEE_{0.71}$-3k	71	3.4	1.01	98.2	0.9057	66	1.42
1,2-$PBD_{0.5}$-*co*-$hPEE_{0.5}$-7k	50	6.8	1.01	98.2	0.8788	127	
1,2-$PBD_{0.63}$-*co*-$hPEE_{0.37}$-25k	37	25	1.04	99.3	0.8800	478	
1,2-$PBD_{0.8}$-*co*-$hPEE_{0.2}$-25k	20	25	1.04	99.3	0.8800	478	
d($PE_{0.21}$-*co*-$PEE_{0.79}$)-3k	79	2.6	1.05	79	0.9291	49	3.31
d($PE_{0.58}$-*co*-$PEE_{0.42}$)-2k	42	2.4	1.02	42	0.8921	48	2.76
d($PE_{0.79}$-*co*-$PEE_{0.21}$)-3k	21	3.4	1.05	21	0.8957	68	2.48
d($PE_{0.95}$-*co*-$PEE_{0.05}$)-3k	5	2.8	1.05	5	0.9833	52	3.29

[a] 1,2-PBD_a-*co*-$dPEE_{1-a}$-*X*k and 1,2-PBD_b-*co*-PEE_{1-b}-*Y*k refer to 1,2-PBD-*co*-PEE copolymers (obtained through saturation of 1,2-PBD with D_2 and H_2, respectively), with $(1 - a)$ and $(1 - b)$ vol fractions of PEE units and M_w of *X* and *Y* kg/mol. d(PE_c-*co*-PEE_{1-c})-*X*k refers to the deuterated PE-*co*-PEE copolymer with $(1 - c)$ vol fraction of PEE units and M_w of *X* kg/mol. [b] Vol % PEE in 1,2-PBD-*co*-PEE or PE-*co*-PEE measured through ^{1}H NMR; error estimated at ±0.4–0.9%. [c] Measured for the PBD precursor using GPC with light scattering. [d] % 1,2-addition of the PBD precursor. Measured through ^{1}H NMR; error estimated at ±0.4–0.9%. [e] Measured using the density gradient column. The error was quantified through multiple measurements in multiple columns and was ±0.0001–0.0003 g/mL. [f] Number of repeat units per chain at 23 °C based on a reference volume of 100 Å^3. An average thermal expansion coefficient of 0.00068 K^{-1} was used for the polymers to account for the temperature dependence of the molar volume.[24,25] [g] The number of deuterium atoms per repeat unit was calculated following eq 2.

Table 3. Blend Characteristics

blend	component 1: 1,2-PBD-*co*-PEE, 1,2-PBD or PE-*co*-PEE[a]	component 2: 1,4-PI[b]	ϕ_1[c]	$T_{c,SANS}$[d] (°C)
hPEE-5k/d1,4-PI-3k	hPEE-5k	d1,4-PI-3k	0.42	34 ± 2
dPEE-3k/1,4-PI-3k	dPEE-3k	1,4-PI-3k	0.51	48 ± 3
1,2-$PBD_{0.2}$-*co*-$dPEE_{0.8}$-47k/1,4-PI-3k	1,2-$PBD_{0.2}$-*co*-$dPEE_{0.8}$-47k	1,4-PI-3k	0.80	78 ± 3
1,2-$PBD_{0.29}$-*co*-$dPEE_{0.71}$-3k/1,4-PI-11k	1,2-$PBD_{0.29}$-*co*-$dPEE_{0.71}$-3k	1,4-PI-11k	0.36	<25
1,2-$PBD_{0.5}$-*co*-$hPEE_{0.5}$-7k/d1,4-PI-23k	1,2-$PBD_{0.5}$-*co*-$hPEE_{0.5}$-7k	d1,4-PI-23k	0.39	<25
1,2-$PBD_{0.63}$-*co*-$hPEE_{0.37}$-25k/d1,4-PI-23k	1,2-$PBD_{0.63}$-*co*-$hPEE_{0.37}$-25k	d1,4-PI-23k	0.51	<25
1,2-$PBD_{0.8}$-*co*-$hPEE_{0.2}$-25k/d1,4-PI-23k	1,2-$PBD_{0.8}$-*co*-$hPEE_{0.2}$-25k	d1,4-PI-23k	0.51	>170 (LCST)
1,2-PBD-47k/d1,4-PI-23k	1,2-PBD-47k	d1,4-PI-23k	0.60	>170 (LCST)
d($PE_{0.21}$-*co*-$PEE_{0.79}$)-3k/1,4-PI-4k	d($PE_{0.21}$-*co*-$PEE_{0.79}$)-3k	1,4-PI-4k	0.51	90 ± 10
d($PE_{0.58}$-*co*-$PEE_{0.42}$)-2k/1,4-PI-4k	d($PE_{0.58}$-*co*-$PEE_{0.42}$)-2k	1,4-PI-4k	0.49	<80
d($PE_{0.79}$-*co*-$PEE_{0.21}$)-3k/1,4-PI-2k	d($PE_{0.79}$-*co*-$PEE_{0.21}$)-3k	1,4-PI-2k	0.55	90 ± 10
d($PE_{0.95}$-*co*-$PEE_{0.05}$)-3k/1,4-PI-2k	d($PE_{0.95}$-*co*-$PEE_{0.05}$)-3k	1,4-PI-2k	0.57	105 ± 5

[a] 1,2-PBD-*co*-PEE copolymers and (h/d)PEE homopolymers were obtained through saturation of 1,2-PBD with H_2 or D_2. 1,2-PBD was obtained through anionic polymerization of 1,3-butadiene. d(PE-*co*-PEE) copolymers were obtained through saturation of 1,4-PBD-*co*-1,2-PBD copolymers with D_2. [b] The protonated 1,4-PI was obtained through anionic polymerization of isoprene. The deuterated 1,4-PI (d1,4-PI) was purchased from Polymer Source. [c] Blend compositions were at the critical compositions calculated by Flory–Huggins (F–H) theory for all blends except for blend hPEE-5k/d1,4-PI-3k whose critical composition ϕ_1^c is 0.32. [d] Temperature at which the sample transitioned from the single-phase state to the two-phase state, as observed through SANS. Blends exhibited upper critical solution temperature (UCST) behavior unless specified as LCST (lower critical solution temperature). For all blends except hPEE-5k/d1,4-PI-3k, this is the critical temperature (T_c) as they were prepared at their critical composition. The error was quantified from the temperature increments used in the SANS experiments, e.g., if data were collected in 10 °C increments, and then the error was quantified as ±°5 C.

$$ {}_{g\,i} \quad \alpha \quad {}_{g\,i\ \mathrm{theor}} \tag{3} $$

where $R_{g,\,i,\,\mathrm{theor}}$ was calculated from literature values of l_i, converted to the basis of $v_{ref} = 100$ Å^3 (l_i = 6.0, 5.7, 7.7, and 4.7 Å for 1,2-PBD, 1,4-PI, PE, and PEE, respectively, at 30 °C).[27−30] The adjustable fit parameters were χ and as the SANS data were fitted with the RPA model at each temperature.

For 1,2-PBD-*co*-PEE and PE-*co*-PEE copolymers, the statistical segment length, l_i, was calculated based on an empirical formula that was previously validated in poly(-olefin-*co*-ethylene) random copolymers as well as random copolymers of 1,4 and 1,2-PBD across a range of copolymer compositions:[14,18,31]

$$ l \quad \sum^{k} l x \tag{4} $$

where l_i and x_i are the statistical segment length and volume fraction (in the copolymer) of each type of repeat unit, comprising a copolymer with k units.

2.4. Data Interpretation. The χ parameters extracted from the Zimm and RPA analyses of SANS data were interpreted using RCT (eq 1) and more advanced models described below that include contributions due to differences in the monomer structure of blend components, nonrandom mixing, and differences in the response to temperature and pressure of the volumetric properties of the pure components of the blends. We emphasize that variations in copolymer composition (x and y in eq 1) are distinct from changes in blend composition (volume fraction of each component i in the blend, ϕ_i). We are not exploring effects of blend composition in this paper.

2.4.1. Lattice Cluster Theory. The lattice cluster theory (LCT) proposed by Freed and co-workers quantifies the influence of monomer structure that causes nonrandom mixing effects on thermodynamic interactions of binary polymer blends (described in more detail in the Supporting Information).[32] As an extension of F–H theory, the LCT describes interactions between united atom groups and includes a temperature-independent contribution. LCT was successfully applied to describe the thermodynamic properties of polymer blends including those of norbornene-*co*-ethylene random copolymer mixtures where the data depart significantly from the predictions of traditional RCT based on F–H theory.[33] LCT connects the F–H χ with parameters that describe the monomer structure.